



Contents lists available at ScienceDirect

Journal of Biomechanics

journal homepage: [www.elsevier.com/locate/jbiomech](http://www.elsevier.com/locate/jbiomech)  
[www.JBiomech.com](http://www.JBiomech.com)

## Effects of the basic multicellular unit and lamellar thickness on osteonal fatigue life

George Pellegrino<sup>a</sup>, Max Roman<sup>b</sup>, J. Christopher Fritton<sup>a,c,\*</sup><sup>a</sup> Department of Orthopaedics & Graduate School of Biomedical Sciences, New Jersey Medical School, Rutgers University, 205 South Orange Avenue, Newark, NJ 07103, USA<sup>b</sup> Department of Biomedical Engineering, New Jersey Institute of Technology, 323 Martin Luther King, Jr. Boulevard, University Heights, Newark, NJ 07102, USA<sup>c</sup> Department of Biomedical Engineering, School of Engineering, Rutgers University, 599 Taylor Road, Piscataway, NJ 08854, USA

### ARTICLE INFO

#### Article history:

Accepted 13 June 2017

Available online xxxxx

#### Keywords:

Osteon  
Lamella  
Interstitium  
Remodeling

### ABSTRACT

A remodeling cycle sets the size of the osteon and associated lamellae in the basic multicellular unit. Treatments and aging affect these micro-structural features. We previously demonstrated decreased fatigue life with an unexplained mechanism and decreased osteon size in cortical bone treated with high-dose bisphosphonate. Here, three finite element models were examined: type-1: a single osteon, as a homogeneous unit and with heterogeneous lamellae and interlamellae, type-2: a control, interstitial-only tissue and type-3: the osteon with cement line, set within the interstitial tissue. Models were loaded in simulated, sinusoidal bending fatigue. As osteon size was decreased, lamellar number and lamellar thickness were incrementally adjusted for each model. As hypothesized, lamellae within the larger type-1 models attained greater cycles to failure and the addition of an osteon to type-2 models (generating a type-3 model set) yielded increased fatigue life. However, as the osteon size was decreased, the potential for compressive damage nucleation was increased within the lamellae of the osteons versus the interstitium. Also, osteons with fewer, thicker lamellae displayed increased fatigue life. Osteonal microstructure plays a role in damage initiation location, especially when BMU size is smaller. Previous findings by us and others could partially be explained by this further understanding of increased probability for damage nucleation in smaller osteons.

© 2017 Elsevier Ltd. All rights reserved.

### 1. Introduction

Bone remodeling effects tissue damage removal and mechanical property restoration via new tissue (Bajaj et al., 2014; Geissler et al., 2015; Lee et al., 2002; Nalla et al., 2003). Damage occurs primarily through fatigue from daily cyclic activities, presenting as microcracks within the bone microstructure (Diab and Vashishth, 2005; George and Vashishth, 2005; Nalla et al., 2003). The heterogeneous makeup of the bone's microstructure and lower-level hierarchy are generally attributed with the resistance of bone to fatigue and fracture. Remodeling restores heterogeneity, decreasing

the local tissue age in the process (Abdel-Wahab et al., 2012; Ascenzi and Lomovtsev, 2006; Demirtas et al., 2016).

In a remodeling cycle the basic multicellular unit (BMU) first removes tissue (Dempster et al., 2013). An osteoclast-filled cutting cone is followed by osteoblasts in a closing cone that generates a new osteon within the resorbed Howship's cavity. Within cortical bone the osteoblasts form full osteons by Type-1 collagen production in lamellar layers that produce a columnar structure. Each lamella is laid down during one cycle of growth with a size that can be affected by many factors (Bromage et al., 2009). Alterations in osteon structure and/or lamellae have been suggested to influence the load bearing and fatigue resistance of bone in large, long-lived animals, including humans (Ascenzi et al., 2016; Barth et al., 1992; Geissler et al., 2015; Pidaparti and Burr, 1992).

Our group found that osteon cross-sectional size, including wall-width (or diameter), and osteocyte density was smaller after 3-year, high-dose treatment with an anti-resorptive bisphosphonate, alendronate, in the rib of adult, female beagle dogs (Bajaj et al., 2014). Additionally, our results and that of another group indicate that in large animal models, long-term, anti-resorptive

*Abbreviations:* FEA, Finite Element Analysis; BMU, Basic Multicellular Unit; On.Wi, osteon wall width ( $\mu\text{m}$ ); On.Dm, osteon diameter ( $\mu\text{m}$ ); Lm.N, lamellar number; Ir.Lm.N, interlamellar number; Lm.Th, lamellar thickness ( $\mu\text{m}$ ); Ir.Lm.Th, interlamellar thickness ( $\mu\text{m}$ ).

\* Corresponding author at: Department of Orthopaedics, Rutgers, the State University of New Jersey, New Jersey Medical School, CC, G-1216, 205 South Orange Avenue, Newark, NJ 07103, USA.

E-mail address: [chris.fritton@rutgers.edu](mailto:chris.fritton@rutgers.edu) (J.C. Fritton).

<http://dx.doi.org/10.1016/j.jbiomech.2017.06.006>

0021-9290/© 2017 Elsevier Ltd. All rights reserved.

treatment with bisphosphonates decrease cortical bone tissue fatigue life measured *ex vivo* (Bajaj et al., 2014; Brock et al., 2015; Geissler et al., 2015). Bisphosphonates are designed to attenuate bone resorption. This aids in the maintenance of bone mineral density and reduces clinical fracture risk for many. Thus, the 14% smaller osteon area, corresponding to smaller osteon diameter, in our previous study is not surprising, given the restraint on the resorptive phase of the BMU expected with an anti-resorptive agent. An explanation for reduced osteocyte density is not so straightforward and may reflect a reduced proliferation rate of osteoblasts required to fill resorption spaces (Bromage et al., 2009). Osteocytes are believed to be the primary activators of resorption and recent *in vitro* data suggests that regulation by osteocytes may be a means by which bone formation and resorption are maintained in equilibrium (Bonewald, 2010, 2011). An alteration in osteoblast proliferation would be expected to also alter lamellar thickness. A recent study suggests that non-osteoporotic women with low-energy fracture exhibit significant reduction in lamellar width and average single osteon area (Ascenzi et al., 2016). The latter data support previous observations that secondary osteons formed at older ages are smaller than those formed at younger ages (Evans, 1976; Watanabe et al., 1998).

We hypothesized that smaller osteons may provide a partial mechanistic explanation for decreased tissue fatigue life. Specifically, a shift in damage nucleation sites with cyclic loading may result from an increase in relative interstitial volume and result in decreased tissue heterogeneity. Because the BMU's resorption cavity size determines osteon size and thus may alter lamellar thickness or number during refilling, we also investigated whether lamellar properties affect damage nucleation sites during cyclic loading. To explore these influences single osteon cortical units, based on the results of isolated, prepared osteon samples of Ascenzi et al. (1990), were modeled using finite element analysis (FEA), providing independent evaluation for the roles of osteon geometry and lamellar makeup toward damage nucleation.

## 2. Materials and methods

Models were designed in ANSYS Parametric Design Language (APDL) (version 14.0, Academic Research) and run using an Intel Xeon CPU (E3-1240 V2 @ 3.40 GHz) with 16.0 GB RAM (Windows 7 Professional, 64-bit), with additional processing via a nVIDIA Quadro 2000 card (1 GB, 128 GDDR5). All models were meshed with 3-D, 20-node homogeneous (nonlayered) structural solid, tetrahedral elements. To test element size requirements, convergence testing was performed on the most complex of models, with cylindrical osteon and surrounding interstitial volume loaded in simulated 3-point bending. Element number ranged from 34,053 to 749,099 (Fig. 1). The finest mesh (~750,000 elements) was chosen for subsequent models as maximum shear stress at the representative cement line node showed an asymptotic behavior.

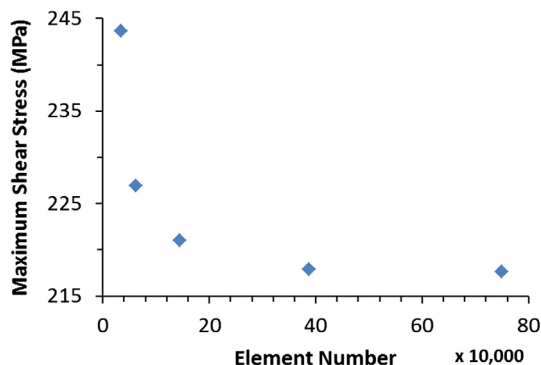


Fig. 1. Convergence in maximum shear stress at the top cement line node (chosen as a representative location) as element number increased. An asymptote was approached as the number of elements utilized in the final models was approached (~750,000).

For the osteons and complexes, the volumes representing individual lamellar and interstitial layers were fully attached at their boundaries to share regions and points that were used by ANSYS to guide the construction of geometry. Thus, the individual elements at the boundary of each layer (and the nodes that define the element geometry) interact as if layers are part of a continuous material, with bonded lamellar, cement line and interstitial regions and no contact-based analysis is performed. Elements within each layer were assigned separate, linear elastic isotropic material properties.

Three model types were designed: type-1: a single osteon alone, as a homogeneous unit with a single elastic modulus and as a unit with each layered lamella containing a unique elastic property, type-2: a homogeneous block of interstitium with a single elastic modulus, with and without an osteonal canal, and type-3: a complex consisting of a layered osteon (type 1), with a cement line centered in a block of interstitium (Fig. 2; Table 1). The single-osteon model was utilized for comparison with the results obtained in quasi-static, monotonic, 3-point bending studies conducted by Ascenzi et al. (1990). Comparison between models of single osteons with and without lamellar structure also provides an estimate for the degree to which lamellar structure influences behavior of the single osteon. Complexes (types 2 and 3) were utilized to explore the effects of osteon presence, wall thickness and lamellar makeup on potential for damage nucleation.

In previous studies, layers appearing dark by microscopy, due to plane-polarized light, are typically referred to as “dark lamellae” or by scanning electron microscopy (SEM) as “thick lamellae.” We termed these “lamellae.” We termed “interlamellae” to refer to “bright lamellae” by polarized, light microscopy or “thin lamellae” by SEM (Ascenzi and Bonucci, 1976; Ascenzi et al., 2003, 2016; Bhushan, 2004; Rho et al., 1999). Lamellar and interlamellar thicknesses ranged from 3–7  $\mu\text{m}$  based on the average reported for osteons from a large range of mammals (Bromage et al., 2009). Unique, individual lamellar and interstitial properties were based on those reported by Hogan, 1992 and Rho et al., 1999 (Table 1). The Rho et al. (1999) data are based on single osteons with 8 “thick” lamellae with a gradation of highest to lowest moduli at innermost and outermost lamellae, respectively. These values agree with average lamellar and interstitial values reported by others (Ascenzi et al., 1990, 2016; Barth et al., 1992; Bhushan, 2004; Bromage et al., 2009; Hengsbarger et al., 2002; Hogan, 1992). The gradient is due to a degree of calcification that is higher near the osteon canal and lower near the cement line. “Thin” interlamellae have a considerably lower modulus and are within the range reported by Hengsbarger et al. (2002).

The 14% decreased osteon area found in our previous study with bisphosphonate treatment was incorporated into the models by decreased osteon diameters and modifications of the lamellae (Bajaj et al., 2014). Thus, for all models, four osteon diameters were chosen: 100%, 96%, 93% and 90% (of 195  $\mu\text{m}$ ) to determine how osteon size affects damage nucleation sites (Table 2). Previous studies have demonstrated differences in osteon wall width (On.W.Wi does not include canal space) within these ranges (92%–95%) for patients experiencing low-energy fractures (Ascenzi et al., 2016; Power et al., 2003). These osteons correspond to those in our study that are 4%–7% smaller by diameter and thus, 8%–14% smaller by cross-sectional area.

As the osteon size decreases two main changes may occur at the lamellar level, either lamellae become thinner or lamellar number decreases. Lamellar variations for each of the different osteon model diameters were designed to address the possible configurations based on the reported ranges for osteons as differences in lamellar thickness were suggested to be associated with increased fragility (low-energy) fracture risk (Ascenzi et al., 2016). Three basic variations were tested where there must be one fewer interlamellar compared to lamellar spaces: (1) 15 lamellae (8 lamellae, 7 interlamellae), (2) 13 lamellae (7 lamellae, 6 interlamellae), and (3) variable number of lamellae dependent on the osteon diameter (Table 2). For variations 1 and 2, the lamellar to interlamellar thickness ratio was 1:1. Thus, this thickness decreased proportionally with the decreased osteon diameter. For variation 3, the lamellar thickness was held as close to constant as possible, with removal of a lamellar/interlamellar pair as their thickness dropped below the minimum of 3  $\mu\text{m}$ . In cases where small adjustments were required the lamellae were decreased in thickness. *In vivo*, lamellae form from the outermost to innermost, thus for 13-lamellar osteons, the modulus for the innermost lamella (lamella 1, Table 1) was not used, to represent the absence of this layer.

For the type-3 models the cement line was assigned a fixed thickness of 5  $\mu\text{m}$  (Hogan, 1992). The interstitial dimensions for the largest osteon occupied approximately 50% of the square cross-section (approximately 237  $\mu\text{m}$   $\times$  237  $\mu\text{m}$ ). The resulting osteon-to-interstitium ratios are within reported ranges (Ascenzi et al., 2016; Bajaj et al., 2014; Geissler et al., 2015). A 500  $\mu\text{m}$  depth is the length of average, isolated, prepared single osteons observed by Ascenzi et al. (1990) to avoid Volkmann's canals that would affect mechanical testing and add large discontinuities to models.

All loads and boundary conditions were also designed to replicate the three-point bending setup used by Ascenzi et al., 1990. Models were loaded in simulated three-point bending (Fig. 3). Constrained and loaded patches (the area over which the load is applied in the model) were matched to Ascenzi et al. for single osteons (50  $\mu\text{m}$   $\times$  237  $\mu\text{m}$  fixed patches at the bottom of each sample and a single centralized 80  $\mu\text{m}$   $\times$  237  $\mu\text{m}$  loading patch at the top). Loads were distributed over the nodes within the loading patch. Due to z-axis symmetry, computational time was reduced by use of models of half the total depth (250  $\mu\text{m}$  total depth).

Download English Version:

<https://daneshyari.com/en/article/5031961>

Download Persian Version:

<https://daneshyari.com/article/5031961>

[Daneshyari.com](https://daneshyari.com)